A New Dynamic Model of the Wheelchair Propulsion on Straight and Curvilinear Level-ground Paths

Félix Chénier, Pascal Bigras, Rachid Aissaoui *†‡

February 4, 2014

Abstract

Independent-Rollers Wheelchair Ergometers (IRE) are commonly used to simulate the behaviour of a wheelchair propelled in straight line. They cannot however simulate curvilinear propulsion. To this effect, a motorized wheelchair ergometer could be used, provided that a dynamic model of the Wheelchair-user system propelled on Straight and Curvilinear paths (WSC) is available. In this paper, we present such a WSC model, its parameter identification procedure and its prediction error. Ten healthy subjects propelled an instrumented wheelchair through a controlled path. Both IRE and WSC models estimated the rear wheels' velocities based on the users' propulsive moments. On curvilinear paths, the outward wheel shows RMS errors of 13% (IRE) vs 8% (WSC). The inward wheel shows RMS errors of 21% (IRE) vs 11% (WSC). Differences between both models are highly significant ($p < 0.001$). A wheelchair ergometer based on this new WSC model will be more accurate than a roller ergometer when simulating wheelchair propulsion in tight environments, where many turns are necessary.

Keywords: Wheelchairs, simulation, dynamics, modelling, ergometers, parameter identification.

1 Introduction

Biomechanical analysis of manual wheelchair propulsion on level ground is often performed on stationary manual wheelchair ergometers. These devices aim to simulate the rear wheel's kinematics and kinetics, so that when the user propels the wheelchair on an ergometer, the rear wheels behave as if the wheelchair was propelled on the ground.

One of the most common stationary ergometers is the roller ergometer, which consists of a device where both rear wheels of a standard wheelchair sit on one or two rollers. These rollers have a certain inertia and resistance that are adjusted to approach the effect of the mass and rolling resistance of the wheelchair-user system. There are however two important dynamic behaviours that are not simulated by the wheelchair ergometers. The first is the movement of the upper body that modifies the rolling resistance during the propulsion cycle and that contributes to the acceleration of the wheelchair during the recovery phase [Sauret et al.(2008)]. This phenomenon cannot be simulated with a purely passive device like a roller ergometer. The second is the propulsion on curvilinear paths. In fact, a common-roller ergometer (one roller shared by both rear wheels) constrains the rear wheels to the same velocity, which prevents curvilinear propulsion [Devillard et al.(2001)]. Besides, an independent-rollers ergometer is built in such a way that each rear wheel has its own velocity [Langbein et al.(1993), Fitzgerald et al.(2006), Yao(2007), Faupin et al.(2008), DiGiovine et al.(2001), Harrison et al.(2004), Niesing et al.(1990), Sasaki et al.(2008)]. However, whereas these ergometers are well adapted to analyze the left-right propulsion asymmetry on straight line [De Groot et al.(2002)], both rear wheels stay uncoupled. The wheelchair-user system is not simulated as a whole, but instead as two independent systems. Thus, curvilinear propulsion is not simulated neither by independent-roller ergometers.

*F. Chénier and P. Bigras are with the Laboratoire de recherche en Imagerie et Orthopédie (LIO), Centre de recherche du Centre hospitalier de l'Université de Montréal (CRCHUM), Montreal, and the Département de génie de la production automatisée, École de technologie supérieure, Montréal.

†R. Aissaoui is with the Laboratoire de recherche en Imagerie et Orthopédie (LIO), CRCHUM, Montreal, with the Département de génie de la production automatisée, École de technologie supérieure, Montréal, and the Centre de recherche inter-disciplinaire en réadaptation de Montréal, Institut de réadaptation Gingras-Lindsay, Montréal.

‡Corresponding author: felix.chenier@etsmtl.ca.

The other most common stationary ergometer is the treadmill ergometer. This ergometer does simulate the dynamic effect of the upper body movement [Vanlandewijck et al.(1994)]; however, propulsion is limited to straight line at a fixed velocity.

Recently, a new kind of roller ergometer designed as a haptic robot was developed [Chénier et al.(2014)]. This ergometer allows to simulate any dynamic behaviour at the interface between the user and the wheelchair's wheels, through the use of haptic control loops controlled by a real-time computer. This new kind of ergometer may eventually solve current ergometers issues, provided that a suitable dynamic model of the wheelchair-user system is available to be simulated in real time.

Very detailed dynamic models of the wheelchair-user system currently exist. For example, [de Saint Rémy(2005)] and [Bascou(2012)] developed detailed models of the user's segments and wheelchair parts. However, these models could not be used readily by the ergometer described in [Chénier et al.(2014)], because the position of the user's body cannot yet be calculated in real time and passed to the dynamic model as an input. This article will thus focus on the second issue with current ergometers, that is the curvilinear aspect of the propulsion. The subject will be assumed to remain still on the wheelchair, and this limitative assumption will be discussed at the end.

To take curvilinear propulsion into account, the dynamic model of the wheelchair-user system must include not only its linear acceleration, but also its angular acceleration. Several dynamic models that consider the user's body as steady and that include both accelerations were developed in the fields of robotics, as velocity controllers for electric wheelchairs [Wang et al.(2009), Shung et al.(1983), Johnson and Aylor(1985)], or path-following controllers for robotic wheelchairs [Miyata et al.(2008), De La Cruz et al.(2010), Coelho and Nunes(2005)]. However, to simplify the identification and control process of these dynamic models, the caster wheels were almost always removed and their contribution to the wheelchair's dynamics was instead considered as an external perturbation. This may be an acceptable compromise for the design of a wheelchair controller; however, when the caster wheels are not aligned with the rear wheels, which is the case in curvilinear propulsion, their contribution on the wheelchair's dynamics is known to be important [Ding et al.(2004), Gentile et al.(1996)]. Thus, the caster wheels should be included in the modelling design.

[Johnson and Aylor(1985)] proposed a dynamic model of the wheelchair that includes the dynamics of the caster wheels. However, they did not explain how they measured the numerous parameters of their model. In fact, some parameters may be difficult to measure, such as the moment of inertia of the wheelchair-user system. As this parameter is strongly related to the user weight and position, it is not available from CAD data. Moreover, experimental measurements need a special setup to make the wheelchair and user rotate or oscillate around the vertical axis [Wang et al.(2007), Eicholtz(2010), Griffiths et al.(2005), Brancati et al.(2010)].

Therefore, there is a need for a dynamic model of the wheelchair that takes both linear and angular accelerations of the wheelchair-user system into account, as well as the contribution of the caster wheels. Moreover, the inertial and friction parameters of the wheelchair-user system must be identified systematically: in fact, it is advisable to automate the estimation of all these parameters, so that for every user, the behaviour of the wheelchair ergometer is entirely defined by mimicking the behaviour of the user's own wheelchair propelled on the ground.

The purpose of this article is three-fold. The first is the development of a new bidimensional dynamic model of a Wheelchair-user system propelled on Straight and Curvilinear level ground paths (WSC). The second is the development of an identification process that estimates the inertial and friction parameters of the WSC model, which are the mass, the rolling resistance and the moment of inertia of the wheelchair-user system. The third is a comparison of the WSC model with the model of a standard Independent-Rollers Ergometer (IRE). This comparison is done by measuring the accuracy of each model in predicting the rear wheels' velocities based on rear wheels' kinetics, for 10 healthy subjects wheeling continuously on both linear and curvilinear level-ground paths.

2 Dynamic models

2.1 IRE model

An independent-rollers ergometer (IRE) is composed of two roller-wheel systems i with a moment of inertia I_{zi} and a moment of rolling resistance M_{Fi} [DiGiovine et al.(1997)], so that:

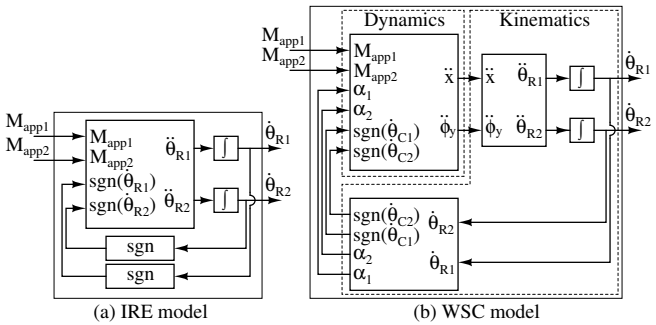

Figure 1: Simulation implementation of both models.

$$I_{zi}\ddot{\theta}_{Ri} = M_{\text{app}i} - \text{sgn}(\dot{\theta}_{Ri})M_{Fi} \tag{1}$$

where $\ddot{\theta}_{Ri}$ and $\dot{\theta}_{Ri}$ are the angular acceleration and angular velocity of the wheel i, and $M_{\text{app}i}$ is the propulsive moment applied on the rear wheel i by the user, which includes the hand torque. To simulate the propulsion of a wheelchair-user system, the inertia and the moment of rolling resistance of each roller-wheel system are adjusted so that:

$$I_{zi} = mr_R^2/2 \tag{2}$$

$$M_{Fi} = r_R F_{\text{roll}}/2 \tag{3}$$

where m is the mass of the simulated wheelchair-user system, r_R is the radius of the rear wheels, and F_{roll} is the total rolling resistance force of the simulated wheelchair-user system.

Replacing (2) and (3) in (1) and converting to a linear acceleration and velocity, we obtain:

$$m\ddot{x} = \sum_i M_{\text{app}i}/r_R - \text{sgn}(\dot{x})F_{\text{roll}} \tag{4}$$

where $\ddot{x}$ and $\dot{x}$ are the anteroposterior acceleration and velocity of the simulated wheelchair-user system relative to the ground. This is the very simple model of the wheelchair-user system that is simulated by an IRE [van der Woude et al.(2001)]. This model is limited by the following assumptions:

Assumption 1 *The wheelchair is always propelled on a straight line.*

Assumption 2 *The movements of the subject on the wheelchair do not contribute to the wheelchair's dynamics.*

Assumption 3 *The rolling resistance force is constant during the analysis.*

Assumption 4 *The air drag is negligible.*

The simulation of an IRE is given by (5). Fig. 1(a) is a block diagram of the simulation implementation of the IRE model.

$$\dot{\theta}_{Ri} = \int \left(\frac{2M_{\text{app}i}}{mr_R^2} - \frac{\text{sgn}(\dot{\theta}_{Ri})F_{\text{roll}}}{mr_R} \right) dt \tag{5}$$

2.2 WSC model

The new WSC model, which was first presented in [Chénier et al.(2011)], is built on assumptions 2.2 to 2.4 of the IRE model, with these additional assumptions:

Assumption 5 *The vertical moment of inertia of the caster wheels and their vertical moment of friction are negligible.*

Assumption 6 *The rolling resistance is due to the caster wheels.*

Assumption 7 *The wheels do not slip on the floor.*

Assumptions 2.5 to 2.7 do not make the WSC model more restrictive than the IRE: they are simply irrelevant for the IRE model because of the much more restrictive assumption 2.1. However, assumption 2.6 may need an explanation. It is known that the rolling resistance of a wheel is inversely proportional to its radius and proportional to the load acting on it [Kauzlarich(1999)]. The front wheels' rolling resistance F_{front} is thus different to the rear wheels' rolling resistance F_{rear}. Let express F_{front} and F_{rear} as a function of the weight distribution x, where $x \in [0, 1]$, 1 being 100 % on the front wheels.

$$F_{\text{front}} = \mu_{\text{front}} x N \tag{6}$$
$$F_{\text{rear}} = \mu_{\text{rear}} (1 - x) N \tag{7}$$
$$F_{\text{roll}} = F_{\text{front}} + F_{\text{rear}} \tag{8}$$

where N is the total weight of the wheelchair-user system, and μ_{front} and μ_{rear} are rolling resistance coefficients of the front and rear wheels. Assuming the difference between μ_{front} and μ_{rear} is mainly due to the radius of the wheel, we get

$$\frac{\mu_{\text{rear}}}{\mu_{\text{front}}} \approx \frac{r_{\text{front}}}{r_{\text{rear}}} \tag{9}$$

where r_{front} and r_{rear} are the radii of the front and rear wheels.

Combining (6) to (9), we obtain an estimation of the individual contribution of the front and rear wheels to the total rolling resistance:

$$\frac{F_{\text{front}}}{F_{\text{roll}}} = \frac{\mu_{\text{front}} x N}{\mu_{\text{front}} x N + \mu_{\text{rear}} (1 - x) N} = \frac{x}{x + r_{\text{front}} / r_{\text{rear}} (1 - x)} \tag{10}$$

On the wheelchair used for this article, which is described later in the experimental method, r_{front} = 7 cm and r_{rear} = 30 cm. According to (10), as the weight distribution on the front wheels can vary from 0.25 to 0.75 during a propulsion cycle [Sauret et al.(2013)], then the contribution of the front wheels to the rolling resistance can vary from about 59 % to 93 % of the total rolling resistance. We conclude that the front wheels are always the main actors in the total rolling resistance. Thus, as the actual load distribution is not available as an input to the dynamic model, we simplify the problem by assuming that all the rolling resistance is due to the front wheels. This being said, as F_{roll} is considered constant and still represents the total rolling resistance, this simplification only has an impact when the wheelchair is turning. Otherwise, the caster wheels and rear wheels are oriented in the same direction, so the model would behave similarly if F_{roll} was either due to the rear wheels only, to the caster wheels only, or to a combination of both.

2.2.1 Dynamic constraints

Fig. 2 represents the free-body diagram of the WSC model. Summing the forces on x and the moments on y around O yields:

$$m\ddot{x} = (M_{\text{app1}} + M_{\text{app2}})/r_R - \frac{F_{\text{roll}}}{2}\left(\text{sgn}(\dot{\theta}_{C1})\cos(\alpha_1) + \text{sgn}(\dot{\theta}_{C2})\cos(\alpha_2)\right) \tag{11}$$

$$I_{0y}\ddot{\phi}_y = \frac{d_{\text{R}}}{2r_R}(M_{\text{app1}} - M_{\text{app2}}) + \frac{d_F F_{\text{roll}}}{4}\left(\text{sgn}(\dot{\theta}_{C2})\cos(\alpha_2) - \text{sgn}(\dot{\theta}_{C1})\cos(\alpha_1)\right) - \frac{d_L F_{\text{roll}}}{2}\left(\text{sgn}(\dot{\theta}_{C2})\sin(\alpha_2) + \text{sgn}(\dot{\theta}_{C1})\sin(\alpha_1)\right) \tag{12}$$

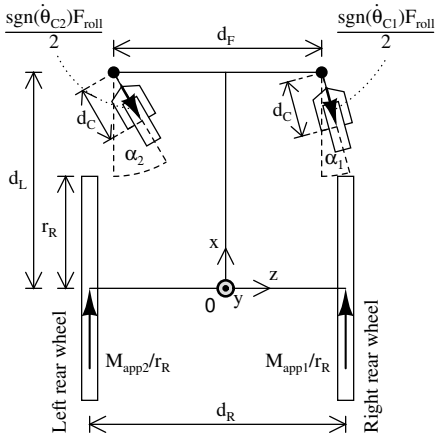

Figure 2: Free body diagram of the WSC model.

where $\ddot{x}$, $\ddot{\phi}_y$ and I_{0y} are the linear acceleration, angular acceleration and vertical moment of inertia of the wheelchair-user system with respect to body frame O. We chose to express the individual rolling resistance forces of each caster wheel as $F_{\text{roll}}/2$ instead of F_{roll} to be consistent with the IRE dynamic model, which models only one rolling resistance force.

2.2.2 Kinematic constraints

According to the wheelchair geometry and to assumption 2.7, the conversion from the wheelchair's linear and angular accelerations ($\ddot{x}$, $\ddot{\phi}_y$) to the rear wheels' angular accelerations ($\ddot{\theta}_{R1}$, $\ddot{\theta}_{R2}$) gives:

$$\ddot{\theta}_{R1,2} = \ddot{x}/r_R \pm \ddot{\phi}_y(d_R/2r_R) \tag{13}$$

Equations (11) and (12) depend on the caster wheels' orientation (α_1, α_2) and on their rolling direction ($\text{sgn}(\dot{\theta}_{C1})$ and $\text{sgn}(\dot{\theta}_{C2})$). It is already known that the caster wheels' rotation rate can be expressed as a first-order differential equation based on the rear wheels' velocities [Chénier et al.(2011)]:

$$\dot{\alpha}_i = \frac{r_R(\dot{\theta}_{R1} - \dot{\theta}_{R2})}{d_C d_R}\left(d_L \cos\alpha_i \mp \frac{d_F \sin\alpha_i}{2} - d_C\right) - \frac{r_R(\dot{\theta}_{R1} + \dot{\theta}_{R2})}{2d_C}\sin\alpha_i, i \in \{1,2\} \tag{14}$$

Also from [Chénier et al.(2011)], the rolling direction of caster wheel i is expressed as:

$$\text{sgn}(\dot{\theta}_{Ci}) = \text{sgn}\{\frac{r_R(\dot{\theta}_{R1} + \dot{\theta}_{R2})}{2}\cos\alpha_i + \frac{r_R(\dot{\theta}_{R1} - \dot{\theta}_{R2})}{d_R}(d_L \sin\alpha_i \pm (d_F/2)\cos\alpha_i)\} \text{ for } i \in \{1,2\} \tag{15}$$

Fig. 1(b) is a block diagram of the simulation implementation of the WSC model.

3 Parameter identification

3.1 IRE model

According to (4), the IRE model is characterized by three parameters, which are the radius of the rear wheels r_R, the system's mass m, and the rolling resistance force F_{roll}. Both r_R and m can be measured

with a measuring tape and a wheelchair-adapted scale, while the rolling resistance F_{roll} can be estimated from different methods. One method is to estimate F_{roll} from the wheelchair deceleration when no forces are applied on the wheels, the deceleration being measured directly with an accelerometer [Bascou et al.(2012)]:

$$F_{\text{roll}} = -m\overline{\ddot{x}} \tag{16}$$

where $\overline{\ddot{x}}$ is the mean value of the wheelchair acceleration during the deceleration.

Another method, which does not implies an accelerometer, is to estimate F_{roll} by a regression of a second order polynomial on the wheelchair position $x(t)$ during the same deceleration [DiGiovine et al.(1997)]:

$$F_{\text{roll}} = -2ma_2 \tag{17}$$

where a_2 is the second order coefficient of the polynomial

$$x(t) \approx a_2 t^2 + a_1 t + a_0 \tag{18}$$

Both methods are interesting because they do not need to derivate the angular position of the wheels, which would generate differential noise. Both methods were used in this work, except for the five subjects where the accelerometer was unavailable.

3.2 WSC model

The new WSC model comprises seven parameters. Four correspond to geometric constants, namely d_F, d_L, d_C and r_R, and three correspond to dynamic constants, namely m, I_{0y} and F_{roll} (each of them being constant according to assumptions 2.2 and 2.3). Whereas the geometric parameters and m can be measured like with the IRE model, and F_{roll} can be estimated by a deceleration test like for the IRE model, I_{0y} cannot be obtained easily. Moreover, to eliminate the need for a scale that is large enough to fit a wheelchair, and to limit the number of operations required to obtain the parameters values, all three parameters m, I_{0y} and F_{roll} will be estimated at once using an offline least-square regression approach.

Estimating m instead of using its real value provides another advantage: the rotation of the rear wheels adds inertia to the system that is not directly taken into account by the WSC model. Therefore, inertial parameters m and I_{0y} will be slightly overestimated so that they include this added inertia. As a consequence, the WSC model will likely be more accurate with an overestimated mass parameter that includes the moment of inertia of the rear wheels, than if a real value was used.

Equations (11) and (12) can be rewritten to isolate the applied moments M_{app1} and M_{app2} and the inertial and friction parameters m, I_{0y} and F_{roll}. We obtain the system $\mathbf{m}_{\text{app}} = \mathbf{W}\mathbf{a}$, where $\mathbf{m}_{\text{app}}$ is the input vector, $\mathbf{W}$ is the state matrix, and $\mathbf{a}$ is the unknown parameters vector:

$$\mathbf{m}_{\text{app}} = \begin{bmatrix} M_{\text{app1}} \\ M_{\text{app2}} \end{bmatrix} \quad \mathbf{a} = \begin{bmatrix} m \\ I_{0y} \\ F_{\text{roll}} \end{bmatrix} \tag{19}$$

$$\mathbf{W} = \begin{bmatrix} \frac{r_R \ddot{x}}{2} & \frac{r_R \ddot{\phi}_y}{d_R} & \frac{r_R}{2}\left(\frac{c_1+c_2}{2} + \frac{d_F(c_1-c_2)}{2d_R} + \frac{d_L(s_1+s_2)}{d_R}\right) \\ \frac{r_R \ddot{x}}{2} & \frac{-r_R \ddot{\phi}_y}{d_R} & \frac{r_R}{2}\left(\frac{c_2+c_1}{2} + \frac{d_F(c_2-c_1)}{2d_R} - \frac{d_L(s_2+s_1)}{d_R}\right) \end{bmatrix} \tag{20}$$

where $c_i = \text{sgn}(\dot{\theta}_{Ci})\cos\alpha_i$ and $s_i = \text{sgn}(\dot{\theta}_{Ci})\sin\alpha_i$, $i \in \{1, 2\}$.

Based on known experimental values for $\mathbf{m}_{\text{app}}$ and $\mathbf{W}$, a least-square regression could be used to estimate $\mathbf{a}$. However, whereas $\mathbf{m}_{\text{app}}$ can be measured directly by instrumented wheels, $\mathbf{W}$ is not directly measurable and needs to be estimated. Therefore, the geometrical parameters r_R, d_R, d_F and d_L will be measured, and the linear acceleration $\ddot{x}$, the angular acceleration $\ddot{\phi}_y$, the caster wheels' orientation α_1, α_2 and the caster wheels' rolling direction $\text{sgn}(\dot{\theta}_{C1}), \text{sgn}(\dot{\theta}_{C2})$ will be estimated.

3.3 State estimation

The linear and angular accelerations $(\ddot{x}, \ddot{\phi}_y)$ of the wheelchair-user system are estimated from the quantized angular positions of the rear wheels ($\hat{\theta}_{R1}$ and $\hat{\theta}_{R2}$), measured by the built-in position encoders at a sampling frequency of 240 Hz. To reject most of the quantification noise, a double-derivative low-pass filter is applied to $\hat{\theta}_{R1}$ and $\hat{\theta}_{R2}$. From the geometry of the wheelchair, the estimated linear and angular accelerations $(\hat{\ddot{x}}, \hat{\ddot{\phi}}_y)$ are given by:

$$\left(g(t) * \hat{\ddot{x}}\right) = \frac{r_R}{2}\left(\ddot{g}(t) * (\hat{\theta}_{R1} + \hat{\theta}_{R2})\right) \tag{21}$$

$$\left(g(t) * \hat{\ddot{\phi}}_y\right) = \frac{r_R}{d_R}\left(\ddot{g}(t) * (\hat{\theta}_{R1} - \hat{\theta}_{R2})\right) \tag{22}$$

where $g(t)$ is the impulse-response of a low-pass filter, $\ddot{g}(t)$ is its second time-derivative, and $*$ is the convolution operator.

Savitzky-Golay filters are particularly powerful in rejecting numerical noise while assessing first and second derivatives [Luo et al.(2005)], which makes it a good candidate for $g(t)$. To use such a filter, the polynomial order and the window size must be optimized. We minimized the root mean square (RMS) error between the real linear acceleration $\ddot{x}$ measured by an accelerometer for five subjects, and the phase-corrected linear acceleration estimated by (21). For a sampling frequency of 240 Hz, the optimized filter was a second-order, 131-points Savitzky-Golay filter.

The caster wheels' orientation α_1, α_2 and the caster wheels' rolling direction $\text{sgn}(\dot{\theta}_{C1}), \text{sgn}(\dot{\theta}_{C2})$ are estimated by (14) and (15). The stability of these differential equations was demonstrated, which allows their use as an observer [Chénier et al.(2011)]. Finally, the filter $g(t)$ must be applied equally on both sides of the equations to match the delay and attenuation introduced by the linear filtering process. Thus, parameters vector $\mathbf{a}$ is estimated by a least-square regression of:

$$(g(t) * \mathbf{m}_{\text{app}}) = (g(t) * \mathbf{W})\,\mathbf{a} \tag{23}$$

on straight and curvilinear propulsion data.

4 Experimental method

The experimental method was approved by the Ethics Committee of the École de technologie supérieure (ÉTS), Montréal, Québec, Canada. Ten healthy young subjects participated in this study. Their anthropometrics are enumerated in Table 1. Data were acquired in a large empty room at ÉTS. The floor was made of flat vinyl tiles. All subjects used the same Ultralight A4 wheelchair (Invacare Corp.) instrumented with two SmartWeels instrumented rear wheels (Three Rivers Holdings, LLC). The weight of the users and that of the wheelchair were measured with an AMTI OR6-7 1000 Force platform (Advanced Mechanical Technology, Inc.). The mass of the instrumented wheelchair was 23.5 kg, including the 5 kg weight of each instrumented wheel. The moment of inertia of each rear wheel along the mediolateral axis was 0.1015 kg·m^2, obtained from CAD data. The angular position of the rear wheels along with the moments applied on them by the subjects were measured at a sampling frequency of 240 Hz. Data analysis and the implementation of the IRE and WSC models were realized with Matlab/Simulink (The MathWorks, Inc.). Additionally, for five of the ten subjects, the linear acceleration of the wheelchair was sampled at 100 Hz with an Inertia Link 3DM-GX2 wireless inertial system (Microstrain, Inc.), which was installed on the middle of the rear wheels' axis.

4.1 Parameter identification

The subjects were asked to familiarize themselves at least 5 minutes with the wheelchair propulsion through the controlled path illustrated in Fig. 3. To identify both models' parameters, the subjects performed the following set of manoeuvres:

Table 1: Subjects' anthropometrics

Subject	Age	Sex	Height (cm)	Weight (kg)	BMI
1	27	M	180	73.5	22.7
2	31	M	173	86.0	28.7
3	25	F	165	67.7	24.9
4	23	M	168	61.9	21.9
5	27	M	169	79.0	27.7
6	23	M	170	63.4	21.9
7	20	M	172	66.8	22.6
8	23	F	162	55.7	21.2
9	26	M	172	86.1	29.1
10	34	M	185	75.9	22.2
Mean	25.9	-	171.6	71.60	24.29
SD	4.1	-	6.8	10.3	3.1

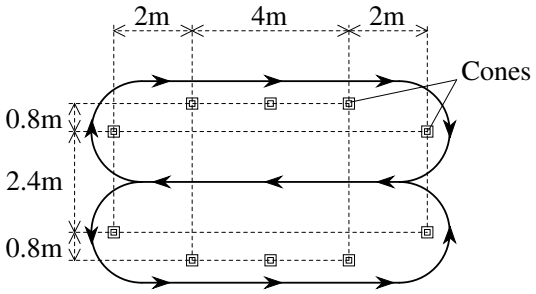

Figure 3: Controlled path of three 6-m straight line sections and four 1-m radius U-turns in both directions.

Dataset 1, sequence 1 From a stop position with the caster wheels trailing behind, the subjects applied one synchronous bilateral push on the rear wheels, and then waited for the wheelchair to stop by itself. This was repeated 10 times.

Dataset 1, sequence 2 Again from a stop position with the caster wheels trailing behind, the subjects applied one unilateral push on a rear wheel, and waited for the wheelchair to stop by itself. This was repeated 10 times with alternating hands.

Dataset 2, sequences 1 and 2 A second set of both sequences was performed to evaluate the repeatability of the parameter identification process.

4.1.1 IRE model

The rolling resistance was estimated using (16) and (17) based on deceleration data from dataset 1, sequence 1.

4.1.2 WSC model

The three inertial and friction parameters (m, I_{0y} and F_{roll}) were estimated using (23) based on propulsion data from dataset 1, sequences 1 and 2. As a goodness-of-fit measure, the coefficient of determination R^2 was calculated for each identification. To evaluate the repeatability of the identification process, the parameters were estimated once more from dataset 2. A test-retest was then performed on each estimated parameter. To this end, the Pearson's correlation coefficient was calculated between the estimated parameters from both datasets.

4.2 Wheel velocity estimation

To compare the angular wheel velocity estimation errors of the IRE and WSC models, the subjects were asked to propel the instrumented wheelchair continuously through the controlled path of Fig. 3. The wheeling speed was controlled at approximately 1 m/s, which corresponds to a normal wheeling speed [Tolerico et al.(2007)], by measuring the time required to complete a lap.

Parameters of both models were identified. For the IRE model, the value of F_{roll} was estimated from the rear wheels position encoders (Eq. 17), because this value was available for all subjects. The rear wheels' angular velocities were then estimated by both models based on the recorded moments. For each propulsion cycle, the RMS velocity error was calculated on a complete push cycle, i.e. from the first hand(s) contact with the hand rim(s) to the next one.

As both models use integrators to estimate the wheel velocities, their outputs are prone to drift due to the integration of modelling errors. To illustrate this drift, Fig. 4a shows an excerpt of the estimated wheel velocities without any correction. To avoid keeping this drift push after push, the estimated kinematics of the wheelchair (the rear wheels angular velocities and the orientation of the caster wheels) were reset to the measured kinematics on each contact between the hand(s) and the hand rim(s). The same excerpt of estimated wheel velocities is shown in Fig. 4b when the drift correction is performed.

The wheel velocity estimation errors of both models were evaluated on four test conditions:

- Left wheel on straight line propulsion
- Right wheel on straight line propulsion
- Outward wheel on curvilinear propulsion
- Inward wheel on curvilinear propulsion

For each test condition, the velocity estimation error $\varepsilon_{1\text{subject}}$ for one subject was obtained by averaging the RMS errors $\varepsilon_{1\text{cycle}}$ on 10 propulsion cycles, according to (24) and (25). Then, the velocity estimation error $\varepsilon_{\text{model}}$ of each dynamic model was calculated as the average error over the 10 subjects (26).

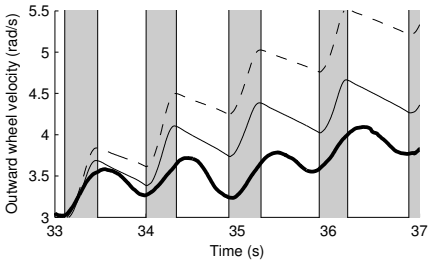

(a) Without drift correction

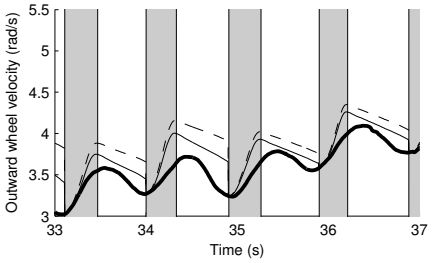

(b) With drift correction

Figure 4: Example of the computed and estimated velocities of the outward wheel on a typical curvilinear continuous propulsion. Computed velocities were obtained from the angular position of the rear wheels filtered at 12 Hz with a 1st order Butterworth filter. Legend:
- - : Estimated velocity, IRE model
— : Estimated velocity, WSC model
— : Computed velocity.
Grey shades correspond to the push phases.

Table 2: Parameters of the IRE model

Subj.	m (measured, kg)	F_{roll} (estimated from wheelchair deceleration, N) Using the position encoders (Eq. 17)	Using the accelerometer (Eq. 16)
1	97.0	13.35	-
2	109.5	16.85	16.49
3	91.2	12.41	11.55
4	85.4	10.24	-
5	102.5	14.01	14.77
6	86.9	12.28	11.18
7	90.3	12.26	-
8	79.2	9.92	-
9	109.6	14.78	-
10	99.4	13.57	13.06

$$\varepsilon_{\text{1cycle}} = \sqrt{\frac{1}{n}\sum_{i=1}^{n}\left\{\left(\frac{\dot{\theta}_{i(\text{estimated})} - \dot{\theta}_{i(\text{measured})}}{\dot{\theta}_{i(\text{measured})}}\right)^2\right\}} \times 100\% \tag{24}$$

where n is the number of samples in the propulsion cycle.

$$\varepsilon_{\text{1subject}} = \overline{\varepsilon_{\text{1cycle}}} \text{ over 10 propulsion cycles} \tag{25}$$

$$\varepsilon_{\text{model}} = \overline{\varepsilon_{\text{1subject}}} \text{ over 10 subjects} \tag{26}$$

$\varepsilon_{\text{model}}$ was compared between the IRE and WSC models for each test condition, and the statistical significance of the difference was tested by a paired t-test applied on the 10 values of $\varepsilon_{\text{1subject}}$.

4.3 Sensitivity analysis

To measure the individual influence of each parameter on the WSC model's $\varepsilon_{\text{model}}$, parameters m, I_{0y} and F_{roll} were varied individually on intervals of $\{-20\%, -10\%, 0\%, +10\%, +20\%\}$ from their estimated value.

5 Results

5.1 Parameter identification

Table 2 shows the parameters of the IRE model, which are the measured mass of the user and wheelchair and the estimated rolling resistance force F_{roll} obtained from wheelchair deceleration. F_{roll} values were similar when estimated from the position encoders and from the accelerometer, with a mean discrepancy of 0.41 ± 0.72 N. This suggests that both methods are equivalent to estimate F_{roll}, and from now on, only F_{roll} computed from the position encoders will be considered.

As the experiments were performed with the same wheelchair and floor, we expected the coefficient of friction μ to be similar for everyone. This was verified, with $\mu = F_{\text{roll(estimated)}} / (m_{\text{measured}} \cdot g) = (13.84 \pm 0.92) \times 10^{-3}$, where g is the gravitational acceleration (9.81 m/s^2).

Table 3 shows the parameters of the WSC model, which are the estimated mass of the user and wheelchair, the estimated vertical moment of inertia, and the estimated rolling resistance force for each subject. The average estimated mass over both data sets was 99.0 ± 12.7 kg, whereas the average measured mass was 95.1 ± 10.3 kg. The mass estimation error was calculated for each subject over both datasets, and showed an average of $4.18 \pm 8.61\%$. The inertial effect of the rear wheels could have contributed to this overestimation,

Table 3: Estimated parameters of the WSC model

Subj.	Param	Data set 1			Data set 2		
		Value (SI)	Error (%)	R^2	Value (SI)	Error (%)	R^2
1	m (kg)	110.81	14.26	0.92	108.56	11.94	0.92
	I_{0y} (kg·m^2)	8.01	-		7.78	-	
	F_{roll} (N)	14.92	-		13.89	-	
2	m (kg)	114.78	4.84	0.90	119.65	9.29	0.91
	I_{0y} (kg·m^2)	9.73	-		7.44	-	
	F_{roll} (N)	18.62	-		18.96	-	
3	m (kg)	90.28	-0.99	0.88	91.37	0.21	0.89
	I_{0y} (kg·m^2)	8.25	-		6.84	-	
	F_{roll} (N)	14.72	-		13.70	-	
4	m (kg)	82.29	-3.61	0.88	75.75	-11.28	0.88
	I_{0y} (kg·m^2)	6.30	-		6.23	-	
	F_{roll} (N)	12.96	-		10.57	-	
5	m (kg)	98.49	-3.89	0.77	85.02	-17.04	0.79
	I_{0y} (kg·m^2)	5.86	-		4.21	-	
	F_{roll} (N)	12.04	-		10.60	-	
6	m (kg)	94.74	9.04	0.92	99.70	14.76	0.81
	I_{0y} (kg·m^2)	6.28	-		6.18	-	
	F_{roll} (N)	13.46	-		15.26	-	
7	m (kg)	94.61	4.79	0.93	95.17	5.42	0.93
	I_{0y} (kg·m^2)	6.82	-		6.07	-	
	F_{roll} (N)	11.43	-		12.20	-	
8	m (kg)	85.63	8.15	0.92	88.12	11.29	0.93
	I_{0y} (kg·m^2)	6.71	-		6.35	-	
	F_{roll} (N)	10.89	-		11.60	-	
9	m (kg)	106.46	-2.85	0.88	116.65	6.45	0.91
	I_{0y} (kg·m^2)	7.40	-		8.55	-	
	F_{roll} (N)	17.45	-		17.62	-	
10	m (kg)	109.93	10.61	0.93	111.49	12.19	0.93
	I_{0y} (kg·m^2)	7.93	-		7.97	-	
	F_{roll} (N)	14.60	-		15.28	-	

adding the equivalent of:

$$m_{\text{equiv}} = 2 \times I_{\text{wheel}}/r_R^2 \tag{27}$$

$$= 2 \times 0.1015/0.3^2 = 2.26 \text{ kg} \tag{28}$$

to the real mass of the system.

As for F_{roll} values obtained from wheelchair deceleration, the mean coefficient of friction was calculated from the estimated values of F_{roll}, and gave $\mu = F_{\text{roll(estimated)}}/\left(m_{\text{estimated}} \cdot g\right) = (14.41 \pm 1.50) \times 10^{-3}$. As expected, it was generally constant over all subjects. Moreover, we expected the estimated values of F_{roll} to be similar to those obtained from wheelchair deceleration. Effectively, a comparison between both models' estimated F_{roll} based on dataset 1 showed a discrepancy of only 1.14±1.50 N. The average estimated moment of inertia over both data sets was 7.05 ± 1.21 kg·m^2.

The average coefficient of determination R^2 was 0.892. This means that generally, 89% of the variance of the applied moments was well modelled, and only 11% was left as residuals. The test-retest for the WSC model's estimated parameters gave Pearson's correlation coefficients of 0.90, 0.67 and 0.89 for m, I_{0y} and F_{roll} respectively. As the minimal correlation coefficient for a 95% confidence with 10 samples is 0.6319 [Fisher et al.(1990)], we conclude that the proposed identification process is repeatable.

5.2 Wheel velocity estimation

Table 4: Wheel angular velocity estimation error $\varepsilon_{1\text{subject}}$ on four test conditions of continuous propulsion (mean ± SD, %)

Subject	Left wheel (straight line)		Right wheel (straight line)		Outward wheel (curvilinear)		Inward wheel (curvilinear)	
	IRE	WSC	IRE	WSC	IRE	WSC	IRE	WSC
1	5.3 ± 2	4.5 ± 1	5.6 ± 2	4.8 ± 1	11.6 ± 5	7.3 ± 3	15.7 ± 12	8.2 ± 6
2	7.2 ± 1	7.7 ± 1	5.8 ± 1	6.2 ± 2	15.0 ± 5	6.1 ± 2	27.3 ± 6	12.6 ± 4
3	5.2 ± 1	5.1 ± 1	6.7 ± 2	6.0 ± 2	11.3 ± 4	5.6 ± 2	17.2 ± 11	7.8 ± 4
4	5.9 ± 1	7.0 ± 2	7.0 ± 4	7.4 ± 3	11.7 ± 6	8.0 ± 4	14.5 ± 8	9.0 ± 4
5	5.1 ± 2	5.5 ± 2	5.6 ± 2	5.4 ± 1	10.6 ± 5	10.0 ± 5	18.0 ± 11	11.3 ± 5
6	5.1 ± 1	5.4 ± 1	4.5 ± 2	4.2 ± 2	8.1 ± 6	5.0 ± 2	18.9 ± 15	10.5 ± 8
7	4.5 ± 1	4.2 ± 1	4.4 ± 1	4.0 ± 1	14.3 ± 6	10.1 ± 4	30.8 ± 19	18.1 ± 11
8	8.5 ± 7	5.1 ± 3	9.3 ± 6	6.6 ± 3	13.3 ± 5	8.8 ± 3	11.8 ± 8	5.8 ± 4
9	8.8 ± 3	10.0 ± 3	7.1 ± 3	7.6 ± 3	16.2 ± 6	9.6 ± 3	26.0 ± 12	15.5 ± 6
10	4.8 ± 1	5.1 ± 1	4.7 ± 2	4.5 ± 1	17.6 ± 2	9.2 ± 2	27.0 ± 17	8.8 ± 6
$\varepsilon_{\text{model}}$	6.04	5.95*	6.06	5.67*	12.98	7.98†	20.73	10.76†
SD	1.58	1.77	1.49	1.31	2.86	1.87	6.48	3.77

* Difference is not significant ($p > 0.05$) † Difference is significant ($p < 0.001$)

Table 4 shows the rear wheels angular velocity estimation errors $\varepsilon_{1\text{subject}}$ and $\varepsilon_{\text{model}}$ for the IRE and WSC models on the four test conditions. On straight line propulsion, the mean error for the WSC model was only 0.09% lower (left wheel) and 0.39% lower (right wheel) than for the IRE model. There was no statistically significant difference between both models.

However, on curvilinear paths, the outward wheel showed an error of 7.98% for the new WSC model, compared to 12.98% for the IRE model. The inward wheel showed an error of 10.76% for the WSC model, compared to 20.73% for the IRE model. Thus, the WSC model reduced the estimation error by half in comparison to the IRE model. The difference between both models was statistically highly significant ($p < 0.001$).

5.3 Sensitivity analysis

Fig. 5 illustrates the sensitivity of the WSC model to a variation of its parameters. For straight line propulsion, we observed that apart when the mass parameter m was largely underestimated (−20%), its variation had little influence on $\varepsilon_{\text{model}}$. Moreover, a variation of both other parameters had no significant effect on $\varepsilon_{\text{model}}$.

On curvilinear propulsion, an underestimation of the mass parameter m also increased $\varepsilon_{\text{model}}$ for both wheels. The moment of inertia parameter I_{0y} was however the most sensitive parameter; moreover, for both wheels, a higher I_{0y} would have increased the accuracy of the simulation. Finally, a variation of the rolling resistance parameter F_{roll} had an opposite effect on $\varepsilon_{\text{model}}$ for the outward wheel versus the inward wheel.

6 Discussion

6.1 Parameter identification

The coefficient of determination R^2 showed that the WSC model fitted well to the propulsion data during the parameter estimation manoeuvres. For a majority of subjects, the estimated mass was also close to the real one, although slightly overestimated, possibly due to the inertial effect of the rotation of the rear wheels.

The estimated coefficient of friction was similar for every subjects, independently of their weight. This was expected as every subjects used the same wheelchair on the same floor. For every subjects, the estimated

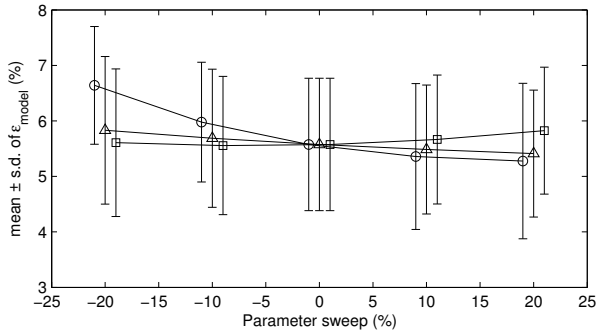

(a) Right wheel on straight line propulsion (left wheel shows similar behavior)

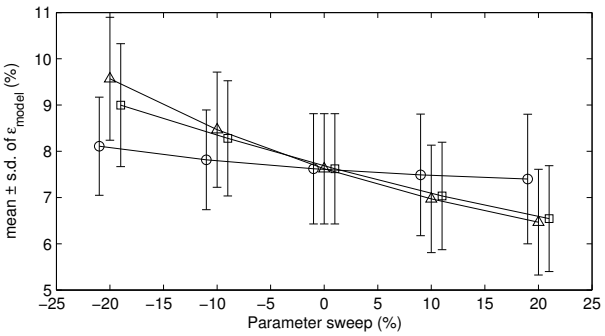

(b) Outward wheel on curvilinear propulsion

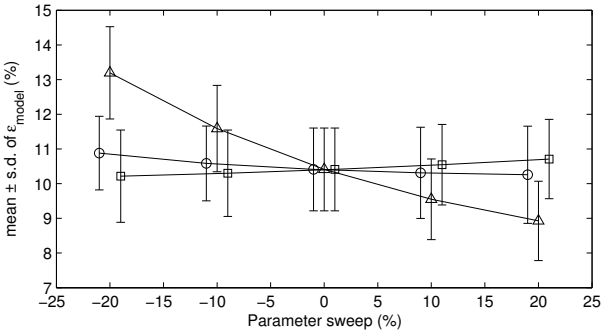

(c) Inward wheel on curvilinear propulsion

Figure 5: Sensitivity of the WSC model to a variation of its parameters: m = ○, I_{0y} = △, F_{roll} = □. The curves are translated on the x-axis on a ±1 interval for clarity.

parameter F_{roll} was similar between the deceleration test and the WSC model's parameter identification process. [Hoffman et al.(2003)] found the coefficients of friction to vary between 1.3×10^{-3} and 15.0×10^{-3} on floors from linoleum to carpet. The average coefficient of friction found in our study was 14×10^{-3}, which falls into this range.

The accuracy of the estimated moment of inertia was difficult to evaluate because no reference value was available. Nevertheless, [Eicholtz(2010)] quantified a Quickie GT (Sunrise Medical, LCC) manual wheelchair's moment of inertia to be 1.213 $\text{kg} \cdot \text{m}^2$ around its centre of mass. Given that this wheelchair weighted 13.17 kg and that its centre of mass was 0.035 m forward to the middle of the rear wheels axis (reference frame O in Fig. 2), the Huygens-Steiner theorem gives a moment of inertia of 1.229 $\text{kg} \cdot \text{m}^2$ around reference frame O. Moreover, [Griffiths et al.(2005)] measured a 3.61 $\text{kg} \cdot \text{m}^2$ moment of inertia for a seated human around his centre of mass. Given that the centre of mass of the user is also forward relative to reference frame O, his moment of inertia around reference frame O is greater than 3.61 $\text{kg} \cdot \text{m}^2$. Thus, the total vertical moment of inertia around reference frame O should be greater than 4.84 $\text{kg} \cdot \text{m}^2$. Our results gave a mean of 7.05 ± 1.21 $\text{kg} \cdot \text{m}^2$, which was effectively greater but in the same order of magnitude. We however remind that the wheelchair's and subjects' moments of inertia measured in [Eicholtz(2010)] and [Griffiths et al.(2005)] were different from our study.

Finally, the test-retest resulted in an excellent estimation repeatability for m and F_{roll}. For I_{0y}, the correlation coefficient value of 0.67 was over the 95% significance threshold of 0.6319 [Fisher et al.(1990)], but it was clearly lower than for m and F_{roll}, which correlation coefficients values were respectively 0.90 and 0.89. Thus, it seems that the estimation of the moment of inertia is not as repeatable as for both other parameters. This may be due to the flexion of the upper-body and the arms movements during the push phase, which modifies slightly the system's moment of inertia between the start and the end of the push.

6.2 Wheel velocity estimation

The rear wheels velocity estimation results revealed that there was no difference in accuracy between the IRE and WSC models on straight line propulsion, which could be explained by evaluating (11) on this particular condition. As the wheelchair is moving in a straight line, the caster wheels are oriented backward: $\alpha_1 = \alpha_2 = 0°$. Moreover, both caster wheels' angular velocity signs are equal to the sign of the wheelchair's linear velocity: $\text{sign}(\dot{\theta}_{C1}) = \text{sign}(\dot{\theta}_{C2}) = \text{sign}(\dot{x})$. Thus, (11) resolves to (4), which corresponds to the IRE's dynamic equation. Therefore, the WSC model is equivalent to an independent-rollers ergometer for straight line propulsion.

On curvilinear propulsion, however, the WSC model is always more accurate than the IRE model. To compare both models quantitatively, we decided to reset the velocity estimation error at each contact with the hand and the hand rim, as seen in Fig. 4b. Nevertheless, we observe in Fig. 4a that the drift of estimated velocity is more important for the IRE model than for the WSC model; this was always observed on curvilinear propulsion. As this drift is due to the integration of modelling errors, we conclude that even without drift correction, the WSC model is still more accurate than the IRE model on curvilinear propulsion.

On both straight and curvilinear continuous propulsion, we observed that the wheelchair accelerated not only during the push phase, but also during the beginning of the recovery phase while no force was applied on the wheels. This phenomenon is observable in Fig. 4, where the real wheel's velocity still increases just after the push phases. We believe this acceleration of the wheelchair is mainly due to the fore-and-aft movement of the user's upper body: just after the push phase, the trunk begins to extend and the movement of the arms change direction, which creates a forward acceleration of the wheelchair. This phenomenon, which was also reported previously [Sauret et al.(2008)], is not taken into account by the IRE model, nor by the WSC model.

Reversely, the same phenomenon generates a deceleration of the wheelchair in the beginning of the push phase. This could explain why on the push phase, the slope of the real wheelchair's velocity is always lower than the slope of the estimated velocity. More work will thus be necessary to develop a model that includes the user motion, for which the parameters are still systematically identifiable, and that can be simulated in real time in a haptic loop. Additionally, the effect of approximating the rolling resistance as constant and generated only by the caster wheels still needs to be investigated.

6.3 Sensitivity analysis

Sensitivity analysis results showed that a variation of the estimated mass had little influence on the WSC model's accuracy. As the subjects applied only the necessary moments to maintain a constant speed, the wheelchair's accelerations were small, which could explain the low influence of the mass. We therefore expect a variation of the mass parameter to have a much higher impact on the model's accuracy when performing start-up maneuvers, as the wheels' accelerations are strongly related to the mass parameter.

As expected for straight line propulsion, a variation of the moment of inertia had no influence on the WSC model's accuracy. However, it seems that for curvilinear propulsion, a higher value for I_{0y} would give more accurate results. This suggests that I_{0y} might be slightly underestimated. Nevertheless, the estimated values of I_{0y} gave satisfactory results in estimating the rear wheels' velocities, without having to use a rotating pendulum or special instrumentation to obtain I_{0y} directly. This makes the parameter identification process much more straightforward, which is an important feature of the proposed dynamic model.

7 Conclusion

We presented a new dynamic model of the wheelchair-user system propelled on straight and curvilinear level-ground paths, along with an identification method that estimates its three inertial and friction parameters, which are the mass, moment of inertia and rolling resistance. Based on the recorded moments applied on the wheels by ten users performing straight and curvilinear continuous propulsion, we compared the estimated rear wheels' velocities from both IRE and WSC models to measured ones. For straight paths, the IRE and WSC models are equivalent. However, for curvilinear paths, the outward wheel shown an error of 7.98% for the new WSC model, compared to 12.98% for the IRE model; the inward wheel shown an error of 10.76% for the WSC model, compared to 20.73% for the IRE model. The new WSC model is aimed to be simulated in real time by a new wheelchair ergometer designed as a haptic robot. For now, as for a roller ergometer, this new ergometer could not simulate the dynamic effect of the user's movement on his wheelchair. However, using this new model, it is expected to simulate a more accurate wheelchair behaviour for a propulsion in tight environments, where it is impossible to wheel only in a straight line.

Acknowledgment

This work was supported by the Fonds Québécois de Recherche sur la Nature et les Technologies (FQRNT), and by the National Sciences and Engineering Research Council of Canada (NSERC). There is no conflict of interest in this project.

Nomenclature

d_C	Caster wheels' trail.
d_F	Distance between both caster wheels.
d_L	Length of the wheelchair.
d_R	Distance between both rear wheels.
F_{roll}	Rolling resistance force.
$g(t)$	Impulse-response of a 2^{nd} order low-pass filter.
I_{0y}	Vertical moment of inertia of the wheelchair-user system.
I_{wheel}	Mediolateral moment of inertia of a rear wheel.
m	Mass of the wheelchair-user system.
$M_{\text{app}i}$	Moment applied on rear wheel i.
push phase	Part of the propulsion cycle with the hand on the handrim.
recovery phase	Part of the propulsion cycle without the hand on the handrim.
r_R	Radius of the rear wheels.
θ_{Ri}	Angular position of rear wheel i.
$\dot{\theta}_{Ci}$	Angular velocity of caster wheel i.
$*$	Convolution operator.

References

[Bascou(2012)] Bascou J. 2012. Analyse biomécanique pour la compréhension et l'amélioration du fauteuil roulant dans son application au tennis de haut niveau. PhD thesis. École nationale supérieure d'arts et métiers.

[Bascou et al.(2012)] Bascou J, Sauret C, , Pillet H, Vaslin P, Thoreux P, Lavaste F. 2012. A method for the assessment of rolling resistance properties for manual wheelchairs rolling on the field. Computer Methods in Biomechanics and Biomedical Engineering pp. 1–11. To review

[Brancati et al.(2010)] Brancati R, Russo R, Savino S. 2010. Method and equipment for inertia parameter identification. Mech Syst Signal Pr 24(1):29–40.

[Chénier et al.(2011)] Chénier F, Bigras P, Aissaoui R. 2011. A new dynamic model of the manual wheelchair for straight and curvilinear propulsionIn: *Proc of the 12th International Conference on Rehabilitation Robotics (ICORR)*. pp. 1–5.

[Chénier et al.(2011)] ———. 2011. An Orientation Estimator for the Wheelchair's Caster Wheels. IEEE Trans Control Syst Technol 19(6):1317–1326.

[Chénier et al.(2014)] ———. 2014. A new wheelchair ergometer designed as an admittance-controlled haptic robot. IEEE/ASME Trans Mechatronics 19(1):321–328.

[Coelho and Nunes(2005)] Coelho P, Nunes U. 2005. Path-following control of mobile robots in presence of uncertainties. IEEE Trans Robotics 21(2):252–261.

[De Groot et al.(2002)] De Groot S, Veeger DHEJ, Hollander AP, Van derWoude LHV. 2002. Wheelchair propulsion technique and mechanical efficiency after 3 wk of practice. Med Sci Sports Exerc 34(5):756–766.

[De La Cruz et al.(2010)] De La Cruz C, Bastos T, Carelli R. 2010. Adaptive motion control law of a robotic wheelchair. Control Eng Pract 19:113–125.

[de Saint Rémy(2005)] deSaint Rémy N. 2005. Modélisation et détermination des paramètres biomécaniques de la locomotion en fauteuil roulant manuel. PhD thesis. Université Blaise Pascal.

[Devillard et al.(2001)] Devillard X, Calmels P, Sauvignet B, Belli A, Denis C, Simard C, Gautheron V. 2001. Validation of a new ergometer adapted to all types of manual wheelchair. Eur J Appl Physiol 85(5):479–485.

[DiGiovine et al.(2001)] DiGiovine CP, Cooper RA, Boninger ML. 2001. Dynamic calibration of a wheelchair dynamometer. J Rehabil Res Dev 38(1):41–55.

[DiGiovine et al.(1997)] DiGiovine CP, Cooper RA, Dvornak M. 1997. Modeling and analysis of a manual wheelchair coast down protocolIn: *Proc of the 19th IEEE-EMBS Annual Conference*. pp. 1888–1891.

[Ding et al.(2004)] Ding D, Cooper RA, Guo S, Corfman TA. 2004. Analysis of driving backward in an electric-powered wheelchair. IEEE Trans Control Syst Technol 12(6):934 – 943.

[Eicholtz(2010)] Eicholtz M. 2010. Design and analysis of an inertial properties measurement device for manual wheelchairs. PhD thesis. Georgia Institute of Technology.

[Faupin et al.(2008)] Faupin A, Gorce P, Thevenon A. 2008. A wheelchair ergometer adaptable to the rear-wheel camber. Int J Ind Ergon 38(7-8):601–607.

[Fisher et al.(1990)] Fisher R, Bennett J, Yates F. 1990. Statistical methods, experimental design, and scientific inference. Oxford University Press, Oxford.

[Fitzgerald et al.(2006)] Fitzgerald S, Cooper RA, Zipfel E, Spaeth D, Puhlman J, Kelleher A, Cooper RA, Guo S. 2006. The development and preliminary evaluation of a training device for wheelchair users: the GAME Wheels system. Disabil Rehabil: Assistive Technology 1(1):129–139.

[Gentile et al.(1996)] Gentile A, Messina A, Trentadue A. 1996. Dynamic behaviour of a mobile robot vehicle with a two caster and two driving wheel configuration. Vehicle System Dynamics 25(2):89–112.

[Griffiths et al.(2005)] Griffiths I, Watkins J, Sharpe D. 2005. Measuring the moment of inertia of the human body by a rotating platform method. Am J Phys 73:85–93.

[Harrison et al.(2004)] Harrison C, Grant M, Conway B. 2004. Haptic Interfaces for Wheelchair Navigation in the Built Environment. Presence: Teleoperators and Virtual Environments 13(5):520–534.

[Hoffman et al.(2003)] Hoffman M, Millet G, Hoch A, Candau R. 2003. Assessment of wheelchair drag resistance using a coasting deceleration technique. Am J Phys Med Rehab 82(11):880–889.

[Johnson and Aylor(1985)] Johnson BW, Aylor JH. 1985. Dynamic modeling of an electric wheelchair. IEEE Trans Industry Applicat IA-21(5):1284 – 1293.

[Kauzlarich(1999)] Kauzlarich J. 1999. Wheelchair rolling resistance and tire design. Biomedical Aspects of Manual Wheelchair Propulsion: The State of the Art II .

[Langbein et al.(1993)] Langbein W, Robinson C, Kynast L, Fehr L. 1993. Calibration of a new wheelchair ergometer: the wheelchair aerobicfitness trainer. IEEE Trans Neur Syst Rehabil Eng 1(1):49–58.

[Luo et al.(2005)] Luo J, Ying K, He P, Bai J. 2005. Properties of Savitzky-Golay digital differentiators. Digital Signal Processing 15(2):122–136.

[Miyata et al.(2008)] Miyata J, Kaida Y, Murakami T. 2008. v–$\dot{\phi}$-Coordinate-Based Power-Assist Control of Electric Wheelchair for a Caregiver. IEEE Trans Industrial Electronics 55(6):2517–2524.

[Niesing et al.(1990)] Niesing R, Eijskoot F, Kranse R, denOuden A, Storm J, Veeger H, van derWoude L, Snijders C. 1990. Computer-controlled wheelchair ergometer. Med Biol Eng Comput 28(4):329–338.

[Sasaki et al.(2008)] Sasaki M, Kimura T, Matsuo K, Obinata G, Iwami T, Miyawaki K, Kiguchi K. 2008. Simulator for Optimal Wheelchair Design. J Robotics and Mechatronics 20(6):854–862.

[Sauret et al.(2008)] Sauret C, Vaslin P, Dabonneville M, Cid M. 2008. Drag force mechanical power during an actual propulsion cycle on a manual wheelchair. Ingénierie et recherche biomédicale (IRBM) pp. 3–9.

[Sauret et al.(2013)] Sauret C, Vaslin P, Lavaste F, deSaint Remy N, Cid M. 2013. Elsevier; Effects of user's actions on rolling resistance and wheelchair stability during handrim wheelchair propulsion in the field. Medical engineering & physics 35(3):289–297.

[Shung et al.(1983)] Shung J, Stout G, Tomizuka M, Auslander D. 1983. Dynamic modeling of a wheelchair on a slope. J Dynamic Syst Meas Control 105:101–106.

[Tolerico et al.(2007)] Tolerico M, Ding D, Cooper RA, Spaeth D, Fitzgerald S, Cooper RA, Kelleher A, Boninger ML. 2007. Assessing mobility characteristics and activity levels of manual wheelchair users. J Rehabil Res Dev 44(4):561.

[van der Woude et al.(2001)] van derWoude L, Veeger H, Dallmeijer AJ, Janssen T, Rozendaal L. 2001. Biomechanics and physiology in active manual wheelchair propulsion. Med Eng Phys 23(10):713–733.

[Vanlandewijck et al.(1994)] Vanlandewijck YC, Spaepen AJ, Lysens RJ. 1994. WILLIAMS & WILKINS; Wheelchair propulsion efficiency: movement pattern adaptations to speed changes. Medicine and Science in Sports and Exercise 26:1373–1373.

[Wang et al.(2007)] Wang H, Grindle G, Connor S, Cooper RA. 2007. An experimental method for measuring the moment of inertia of an electric power wheelchairIn: *Engineering in Medicine and Biology Society, 2007. EMBS 2007. 29th Annual International Conference of the IEEE*. pp. 4798–4801.

[Wang et al.(2009)] Wang H, Salatin B, Grindle G, Ding D, Cooper R. 2009. Real-time model based electrical powered wheelchair control. Med Eng Phys 31(10):1244–1254.

[Yao(2007)] Yao F. 2007. Measurement and Modeling of Wheelchair Propulsion Ability for People with Spinal Cord Injury. PhD thesis. University of Canterbury.